CANCER DISCOVERY

Telomeric Allelic Imbalance Indicates Defective DNA Repair and Sensitivity to DNA-Damaging Agents

Nicolai J. Birkbak, Zhigang C. Wang, Ji-Young Kim, et al.

Cancer Discovery Published OnlineFirst March 22, 2012.

Published OnlineFirst on March 22, 2012; DOI:10.1158/2159-8290.CD-11-0206

RESEARCH ARTICLE

Telomeric Allelic Imbalance Indicates Defective DNA Repair and Sensitivity to DNA-Damaging Agents

Nicolai J. Birkbak[1,2], Zhigang C. Wang[2,3], Ji-Young Kim[3,6], Aron C. Eklund[1], Qiyuan Li[1,2], Ruiyang Tian[2], Christian Bowman-Colin[2], Yang Li[2], April Greene-Colozzi[2], J. Dirk Iglehart[2,3], Nadine Tung[4], Paula D. Ryan[7], Judy E. Garber[2], Daniel P. Silver[2,3], Zoltan Szallasi[1,5], Andrea L. Richardson[2,3]

Published OnlineFirst on March 22, 2012; DOI:10.1158/2159-8290.CD-11-0206

ABSTRACT

DNA repair competency is one determinant of sensitivity to certain chemotherapy drugs, such as cisplatin. Cancer cells with intact DNA repair can avoid the accumulation of genome damage during growth and also can repair platinum-induced DNA damage. We sought genomic signatures indicative of defective DNA repair in cell lines and tumors and correlated these signatures to platinum sensitivity. The number of subchromosomal regions with allelic imbalance extending to the telomere (N_{tAI}) predicted cisplatin sensitivity *in vitro* and pathologic response to preoperative cisplatin treatment in patients with triple-negative breast cancer (TNBC). In serous ovarian cancer treated with platinum-based chemotherapy, higher levels of N_{tAI} forecast a better initial response. We found an inverse relationship between *BRCA1* expression and N_{tAI} in sporadic TNBC and serous ovarian cancers without *BRCA1* or *BRCA2* mutation. Thus, accumulation of telomeric allelic imbalance is a marker of platinum sensitivity and suggests impaired DNA repair.

SIGNIFICANCE: Mutations in BRCA genes cause defects in DNA repair that predict sensitivity to DNA damaging agents, including platinum; however, some patients without BRCA mutations also benefit from these agents. N_{tAI}, a genomic measure of unfaithfully repaired DNA, may identify cancer patients likely to benefit from treatments targeting defective DNA repair. *Cancer Discov; 2(4);* OF1–OF10. *©2012 AACR.*

INTRODUCTION

Cell lines carrying *BRCA1* or *BRCA2* mutations are more sensitive to killing by the platinum salts cisplatin and carboplatin than are wild-type cells (1, 2). Breast and ovarian cancers in patients carrying *BRCA1* or *BRCA2* mutations are likewise sensitive to platinum-based chemotherapy (3, 4). The majority of breast cancers arising in women with a germline *BRCA1* mutation lack expression of estrogen and progesterone receptors or amplification of the *HER2-neu* gene ("triple-negative"). *BRCA1*-related breast cancers share a number of phenotypic characteristics with sporadic triple-negative breast cancer [TNBC (5–7)]. Both tumor types share a common pattern of genomic abnormalities and have high global levels of chromosomal aberrations, including allelic imbalance (AI), the unequal contribution of maternal and paternal DNA sequences with or without changes in overall DNA copy number (8–10). Because they have in common genomic aberrations suggesting a shared lesion in genomic integrity control, it is reasonable to posit that sporadic TNBC that has accumulated high levels of AI might share the sensitivity to platinum-based chemotherapy that characterizes *BRCA1*-associated cancer.

These observations prompted a clinical trial, Cisplatin-1, in which 28 patients with operable TNBC were treated preoperatively with cisplatin monotherapy. Preoperative treatment in the Cisplatin-1 trial resulted in greater than 90% tumor reduction in 10 of 28 (36%) patients, including pathologic complete response (pCR) in 6 women, 2 of whom had *BRCA1*-associated cancers (11). A second trial, Cisplatin-2, accrued 51 patients with TNBC who received the same preoperative cisplatin regimen as those in Cisplatin-1, but in combination with the angiogenesis inhibitor bevacizumab (12).

The response rate in Cisplatin-2 was similar to that in Cisplatin-1. In the second trial, a greater than 90% tumor reduction was observed in 17 of 44 women (39%) completing treatment. In Cisplatin-2, 8 patients carried a germline *BRCA1* or *BRCA2* mutation, of which 4 patients achieved a pCR or near pCR to the cisplatin–bevacizumab regimen. In both trials, all patients had research sequencing to determine their germline *BRCA1* and *BRCA2* status. We compared the number of various chromosomal abnormalities including AI present in tumor biopsies obtained before therapy to pathologically determined tumor response to cisplatin, alone or in combination with bevacizumab, assessed by examination of the posttreatment surgical specimen.

Chromosomal abnormalities such as regions of AI, other than those resulting from whole chromosome gain or loss, might result from improper repair of DNA double-strand breaks during tumor development. If so, then a genome-wide count of abnormal chromosomal regions in tumors may indicate the degree of DNA repair incompetence, independent of knowledge of any specific causative DNA repair defect. We hypothesized that the number of chromosomal regions of

Authors' Affiliations: [1]Center for Biological Sequence Analysis, Technical University of Denmark, Lyngby, Denmark; [2]Dana-Farber Cancer Institute, [3]Brigham and Women's Hospital, [4]Beth Israel Deaconess Medical Center, [5]Children's Hospital Informatics Program at the Harvard-MIT Division of Health Sciences and Technology (CHIP@HST), and Harvard Medical School, Boston, Massachusetts; and [6]CHA University School of Medicine, Seoul, Republic of Korea; [7]Fox Chase Cancer Center, Philadelphia, Pennsylvania

N.J. Birkbak and Z.C. Wang contributed equally to this work.

D.P. Silver, Z. Szallasi, and A.L. Richardson are senior authors and contributed equally to this work.

Note: Supplementary data for this article are available at Cancer Discovery Online (http://www.cancerdiscovery.aacrjournals.org).

Corresponding Author: Andrea L. Richardson, Dana-Farber Cancer Institute, 450 Brookline Avenue, Smith 936A, Boston, MA 02215. Phone: 617 582 7352; Fax: 617 632 3709; E-mail: arichardson@partners.org

doi: 10.1158/2159-8290.CD-11-0206

Published OnlineFirst on March 22, 2012; DOI:10.1158/2159-8290.CD-11-0206

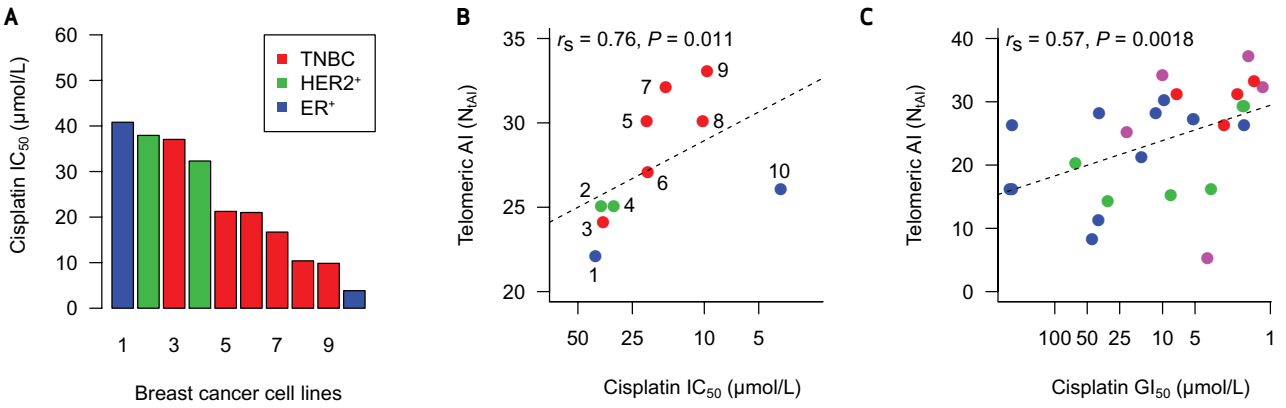

Figure 1. Chromosomal aberrations and cisplatin sensitivity *in vitro*. The relationship between N_{tAI} and cisplatin sensitivity was analyzed in breast cancer cell lines. **A** and **B,** 10 cell lines were included in this study, 1: CAMA-1, 2: HCC1954, 3: MDA-MB-231, 4: MDA-MB-361, 5: HCC1187, 6: BT-549, 7: HCC1143, 8: MDA-MB-468, 9: BT-20, and 10: T47D. **A,** IC_{50} values for each of the 10 cell lines. A proliferation assay was used to assess viability after 48 hours of cisplatin exposure, and IC_{50} was determined from the dose response curves. **B,** relationship between N_{tAI} and cisplatin sensitivity. Breast cancer subtype is indicated as follows: ER^- $HER2^-$, red; $HER2^+$, green, ER^+ $HER2^-$, blue. **C,** relationship between N_{tAI} and cisplatin sensitivity as determined by GI_{50} in breast cancer cell lines from Heiser and colleagues (18). Reported transcriptional subtype is indicated as follows: basal, red; claudin-low, pink; ERBB2Amp, green; luminal, blue. See Supplementary Methods for cell line identifiers.

AI in tumors would predict sensitivity to drugs that induce DNA cross-links such as cisplatin.

We first sought associations between various measures of subchromosomal abnormalities and sensitivity to cisplatin in breast cancer cell lines and found the most accurate predictor to be AI extending to the telomeric end of the chromosome (N_{tAI}). Finally, we tested whether N_{tAI} was associated with treatment response in patient tumor samples in the Cisplatin-1 and Cisplatin-2 TNBC trials and in The Cancer Genome Atlas (TCGA) public data set of serous ovarian cancer, a cancer routinely treated with platinum-based therapy. In an effort to understand more about the processes leading to telomeric AIs, we mapped the location of their breakpoints and observed a striking association of these breakpoints with regions of the genome that are difficult to replicate—common copy number variants (CNV). Furthermore, a subset of high N_{tAI} tumors displays low BRCA1 mRNA levels. These observations begin to suggest models of how telomeric AI may occur.

RESULTS

Cisplatin Sensitivity Correlates with Burden of Telomeric AI in Breast Cancer Cell Lines

We obtained single-nucleotide polymorphism (SNP) genotype array data from the Wellcome Trust Sanger Institute for a set of established *BRCA1* wild-type breast cancer cell lines for which we had determined cisplatin sensitivity [Fig. 1A (13)]. Allele copy number was determined from the SNP array data and AI detected by the use of allele-specific copy number analysis of tumors, or ASCAT [Supplementary Fig. S1 (10)]. We tested for an association between the IC_{50} values for cisplatin and each of 3 summary measures of chromosomal alteration: the number of chromosome regions with AI (N_{AI}; Supplementary Fig. S2A), the number of regions with copy number gains (N_{Gain}; Supplementary Fig. S2B), and the number of regions with copy number loss (N_{Loss}; Supplementary Fig. S2C). None of these measures was correlated with cisplatin sensitivity in the cell lines.

Known defects in DNA double-strand break repair, including loss of BRCA1, cause the spontaneous formation of triradial and quadriradial chromosome structures, which are cytologic indications of aberrant chromosome recombination (14–16). The resolution of these chromosome rearrangements at mitosis can result in large regions of AI and/or copy number changes extending from the cross-over to the telomere (15, 17). More generally, several error-prone repair processes potentially used by cells with defective DNA repair cause chromosome cross-over or copy choice events that result in allelic loss or copy number change extending from the site of DNA damage to the telomere.

We therefore looked for an association between cisplatin sensitivity and the number of contiguous regions of AI, copy gain, or copy loss that either extended to a telomere and did not cross the centromere (telomeric regions) or did not extend to a telomere (interstitial regions; Supplementary Fig. S1, Fig. 1B, and Supplementary Fig. S3). The number of regions of telomeric AI was the only summary genomic measure that was significantly associated with cisplatin sensitivity in the breast cancer cell lines ($r_s = 0.76$, $P = 0.011$; Fig. 1B); the correlation between N_{tAI} and cisplatin sensitivity was stronger when the analysis was restricted to the TNBC lines (Fig. 1B, red circles; $r_s = 0.82$, $P = 0.0499$). A similar relationship was observed between N_{tAI} and cisplatin sensitivity as measured by GI_{50} in a recently published study of breast cancer cell lines [$r_s = 0.57$, $P = 0.0018$; Fig. 1C (18)]. Of all the drugs tested in this study, N_{tAI} was most highly correlated to cisplatin sensitivity.

Tumors Sensitive to Cisplatin-Based Chemotherapy Have Greater Levels of Telomeric AI

We then investigated whether the association between N_{tAI} in clinical tumor samples and cisplatin sensitivity was

Published OnlineFirst on March 22, 2012; DOI:10.1158/2159-8290.CD-11-0206

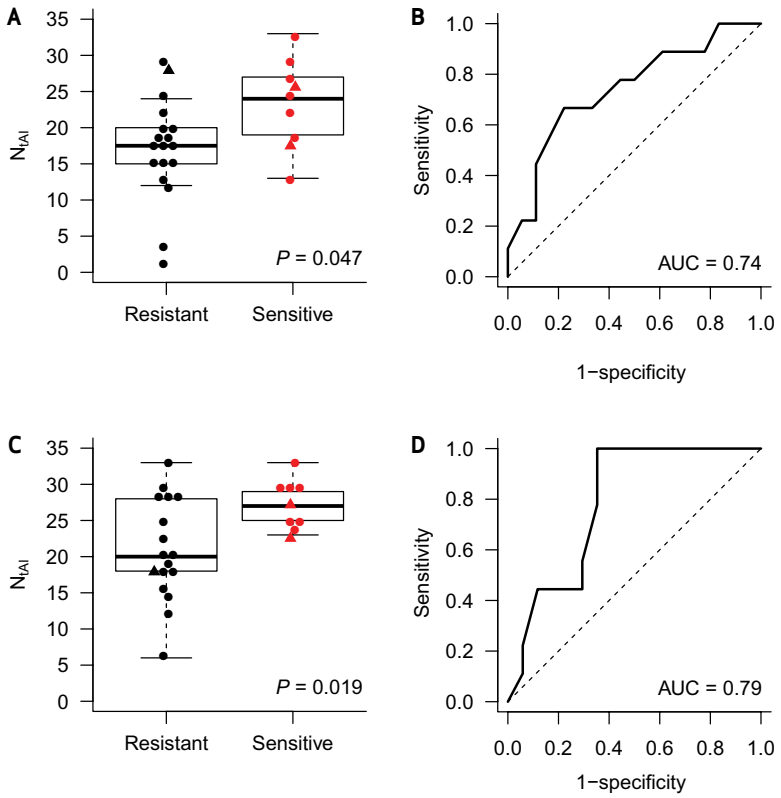

Figure 2. N_{tAI} and cisplatin response in breast cancer. In 2 clinical trials, patients with TNBC were given preoperative cisplatin (Cisplatin-1, **A–B**) or cisplatin and bevacizumab (Cisplatin-2, **C–D**). Cisplatin-resistant tumors are indicated in black; cisplatin-sensitive tumors are indicated in red. Tumors with germline mutations in BRCA1/2 are indicated with triangles. **A** and **C**, box plots showing N_{tAI} distribution in cisplatin-resistant and -sensitive tumors. **B** and **D,** ROC curves showing the ability of N_{tAI} to predict for sensitivity to cisplatin.

present in the Cisplatin-1 trial. Sensitivity was measured by pathologic response determined after preoperative treatment (11). Molecular inversion probe SNP genotype data from pretreatment tumor samples ($n = 27$) were evaluated by ASCAT to determine N_{tAI}. We compared tumors with a reduction of at least 90% in the content of malignant cells (cisplatin-sensitive) to tumors with limited or no response to cisplatin (cisplatin-resistant, defined by tumor reduction of <90%). Cisplatin-sensitive tumors had significantly higher levels of N_{tAI} (median 24 vs. 17.5, $P = 0.047$, Fig. 2A). We tested the ability of N_{tAI} to predict cisplatin response by calculating the area under the receiver operating characteristic (ROC) curve (AUC). ROC analysis showed that higher levels of N_{tAI} were associated with cisplatin sensitivity [AUC = 0.74, 95% confidence interval (CI) 0.50–0.90; Fig. 2B].

In the Cisplatin-2 trial, cisplatin-sensitive tumors ($n = 9$) had significantly greater N_{tAI} than -resistant tumors ($n = 17$, median 27 vs. 20, $P = 0.019$; Fig. 2C). N_{tAI} was also associated with response to cisplatin and bevacizumab by ROC analysis (AUC = 0.79, 95% CI 0.55–0.93; Fig. 2D). The association between N_{tAI} and cisplatin sensitivity remained significant when cases with *BRCA1* or *BRCA2* mutation were excluded and only BRCA normal cases were analyzed ($P = 0.030$ and $P = 0.023$ in Cisplatin-1 and Cisplatin-2, respectively). Therefore, in 2 separate preoperative trials in breast cancer, in which treatment sensitivity was assessed by a quantitative measure of pathologic response, N_{tAI} reliably forecast the response to cisplatin-based treatment.

To test whether the N_{tAI} metric indicates platinum sensitivity in cancers other than breast, we determined the association between N_{tAI} and initial treatment response in a TCGA cohort of serous ovarian cancer patients who had received adjuvant platinum and taxane chemotherapy (19). Among the ovarian cancers without mutation in *BRCA1* or *BRCA2* (wtBRCA), the platinum-sensitive tumors had significantly higher levels of N_{tAI} than did the platinum-resistant cancers (median 22 vs. 20, $P = 0.036$; Fig. 3) and N_{tAI} was predictive of treatment response by ROC analysis (AUC = 0.63, 95% CI 0.50–0.76, Supplementary Fig. S4). The ovarian cancers with somatic or germline mutation in *BRCA1* or *BRCA2* that were sensitive to platinum therapy had even higher levels of N_{tAI} (median = 26, $P = 0.0017$ and median 23.5, $P = 0.037$ vs. resistant wtBRCA, respectively, Fig. 3). All of the *BRCA2*-mutated cancers were platinum sensitive; however, 5 *BRCA1*-mutated tumors were resistant to platinum therapy yet appeared to have relatively high levels of N_{tAI}. Thus, high N_{tAI} is characteristic of serous ovarian cancer with known mutation in either *BRCA1* or *BRCA2*; high N_{tAI} is also found in a subset of sporadic cancers without BRCA mutations, where it is predictive of platinum sensitivity.

Locations of N_{tAI}-Associated Chromosomal Breaks Are Not Random

To develop a better understanding of the processes leading to telomeric AI, we mapped the location of the chromosome breakpoints defining the boundary of the telomeric AI regions. We observed that many breakpoints were located in very close proximity to each other (Supplementary Fig. S5), suggesting a nonrandom distribution of DNA breaks causing telomeric AI. Recurrent chromosomal translocation breakpoints may be associated with regions of repeated

Published OnlineFirst on March 22, 2012; DOI:10.1158/2159-8290.CD-11-0206

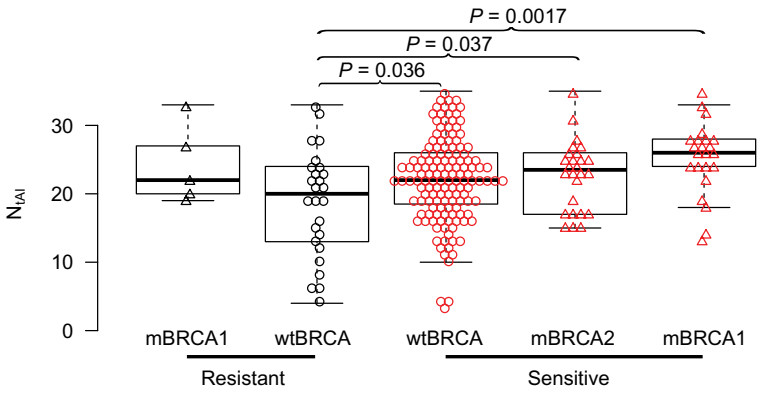

Figure 3. N_{tAI} and cisplatin response in serous ovarian cancer. Box plots showing N_{tAI} distribution in platinum-sensitive and -resistant tumors in cancers without *BRCA1* or *BRCA2* mutations (wtBRCA) and for cancers with germline or somatic mutation in *BRCA1* (mBRCA1) or in *BRCA2* (mBRCA2). Red indicates sensitive samples, and triangles indicate samples with germline or somatic mutations in *BRCA1* or *BRCA2*. Significant differences between resistant wtBRCA and sensitive groups are indicated. In addition, significant differences were found between sensitive wtBRCA and sensitive mBRCA2 ($P = 0.047$), and between sensitive wtBRCA and sensitive mBRCA1 ($P = 0.014$).

DNA sequence that may cause stalled replication forks, an increased frequency of DNA breaks, and subsequent rearrangement by nonallelic homologous recombination or other similar mechanisms (20, 21). CNVs are highly homologous DNA sequences for which germline copy number varies between healthy individuals (22, 23). CNVs have been proposed to facilitate the generation of chromosomal alterations, similar to fragile sites (21, 24, 25).

We compared the number of observed breaks within 25 kB of a CNV to the frequency expected by chance alone on the basis of permuted data. In the Cisplatin-1 cohort, of 517 N_{tAI} breakpoints, 255 (49%) were associated with overlapping CNVs. Similarly, in the cisplatin-2 cohort, of 599 N_{tAI} breakpoints, 340 (57%) were associated with CNVs. In both trials, the observed number of N_{tAI} breaks associated with CNVs was significantly greater than expected by chance (Fig. 4A and B). Thus, many of the breakpoints leading to telomeric AI in TNBC occur near CNVs, suggesting that stalled replication forks, replication stress, or other CNV-associated mechanisms may be involved in the genesis of telomeric AI.

Low BRCA1 mRNA Is Associated with High N_{tAI} and Sensitivity to Cisplatin

In our previous report of the Cisplatin-1 trial, we found an association between low BRCA1 transcript levels and better response to cisplatin (11). In the more recent trial, Cisplatin-2, BRCA1 transcript levels measured by quantitative real-time PCR (qRT-PCR) are also associated with cisplatin response ($P = 0.015$; Fig. 5A). In a combined analysis of data from both trials, lower BRCA1 transcript levels are associated with methylation of the *BRCA1* promoter ($P = 0.027$; Fig. 5B), although *BRCA1* promoter methylation itself is not significantly associated with cisplatin response ($P = 0.25$; Fisher exact test). BRCA1 mRNA levels are inversely associated with N_{tAI} in the 2 cisplatin trials ($r_s = -0.50$, $P = 0.0053$; Fig. 5C). This finding suggests that dysfunction of a BRCA1-dependent process or other abnormality causing low BRCA1 mRNA may be responsible for the high level of telomeric AI and also cisplatin sensitivity in many of these TNBCs.

ROC analysis of the combined TNBC trials suggests that BRCA1 expression level or N_{tAI} may provide a similar predictive accuracy for cisplatin sensitivity (Supplementary Fig. S6A). When high N_{tAI} and low BRCA1 expression are combined in a predictive model, the positive predictive value and specificity of prediction improved considerably, but the sensitivity was decreased relative to N_{tAI} alone (Supplementary Fig. S6B), suggesting that low BRCA1 expression does not account for all cisplatin-sensitive tumors.

In the TNBC trials, we noted a few cisplatin-sensitive tumors with high levels of N_{tAI} but high BRCA1 mRNA, suggesting that alternative mechanisms may drive the generation of tAI in some tumors. Analysis of TCGA data of $ER^-/HER2^-$ breast cancer and wtBRCA serous ovarian cancer reveals an inverse correlation between N_{tAI} and BRCA1 expression. Yet, in both cohorts, there was a considerable subset of tumors with high N_{tAI} and high BRCA1 expression (Supplementary Fig. S7A and B). Unlike N_{tAI}, BRCA1 expression was not apparently different between sensitive and resistant wtBRCA serous ovarian cancers (Supplementary Fig. S7C). These findings suggest a model whereby high N_{tAI} may represent a readout of DNA repair deficiency resulting from either low BRCA1 expression or from other known or unknown mechanisms (Fig. 6).

DISCUSSION

Our study analyzed 2 preoperative clinical trials in women with TNBC treated with cisplatin, in which pathologic response at the time of surgery provided an experimental endpoint. Sporadic TNBCs are heterogeneous in their responses to platinum salts, which are chemotherapeutic agents that depend in part on DNA repair defects for their cytotoxic activity (26, 27). Lesions in DNA repair caused by BRCA1 or BRCA2 dysfunction lead to platinum sensitivity; we reasoned that the types of chromosomal aberrations arising in the context of BRCA dysfunction might also be associated with platinum sensitivity in wtBRCA cancers.

On the basis of results in cell lines, we chose to enumerate one such chromosomal abnormality, telomeric AI, in pretreatment tumor genomes and to relate this to pathologic response after cisplatin therapy. N_{tAI} was associated with response to platinum treatment in our TNBC cisplatin trials and in platinum-treated serous ovarian cancer, and these findings suggest that the burden of this genomic abnormality exposes an underlying deficiency of DNA repair in the

Published OnlineFirst on March 22, 2012; DOI:10.1158/2159-8290.CD-11-0206

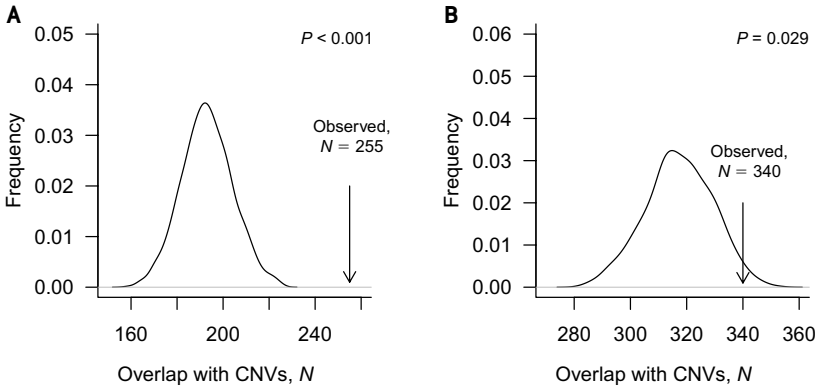

Figure 4. Enrichment of common CNVs in telomeric AI chromosomal breakpoints from TNBC. Association of telomeric AI breakpoints with common CNV loci was determined by computational simulations that compared the expected number of breakpoints containing CNVs with the observed number in total cases in Cisplatin-1 (**A**) and Cisplatin-2 (**B**).

platinum-sensitive subset of these cancers. AI propagated from a given chromosomal location to the telomere suggests the operation of error-prone processes giving rise to abnormal cross-over or template switching events, rather than error-free DNA repair.

We found that the breakpoints of telomeric AI regions are nonrandom and enriched for CNVs. This pattern also suggests defective DNA repair. CNVs are associated with other repeat sequences, such as Alu repeats, are concentrated in pericentromeric and subtelomeric regions, and are associated also with common fragile sites (28, 29). These repeat elements are thought to result in replication "slow zones," which are prone to replication stalling and formation of DNA double-strand breaks (30, 31). Furthermore, downregulation of Rad51 or inhibition of BRCA1 increases the fragility at such sites when cells are under replication stress (32, 33). The observed association of low BRCA1 expression levels in many tumors with high N_{tAI} suggests deficient homologous recombination, impaired S- or G_2–M checkpoint function, or a combination of these factors underlying the generation of this type of genomic abnormality.

Cisplatin forms interstrand cross-links on DNA that lead to stalled replication forks and DNA double-stand breaks that must be repaired if the cell is to survive. It is likely that these breaks are repaired by the use of similar mechanisms to those used at stalled replication forks and DNA breaks generated at sites of CNVs. Therefore, high pretreatment N_{tAI} identifies tumors unable to accurately repair breaks and restart stalled replication forks at sites of CNV. These same tumors are also unable to contend with stalled forks at sites of cisplatin cross-links.

Although AI at sites of CNV may reflect inefficient error-free repair, other explanations should be considered. Both TNBC cohorts showed a significant relationship between N_{tAI} and pathologic response to cisplatin chemotherapy. Nevertheless, there were patients in both trials whose tumors showed poor response to cisplatin therapy despite having high N_{tAI}. Similarly, a few of the *BRCA1*-mutated ovarian cancers had high N_{tAI} yet were resistant to platinum therapy. Because N_{tAI} is a summation of ongoing and past DNA lesions, resistance mechanisms acquired after generation of tAI would confound the relationship between N_{tAI} and response. In carriers of *BRCA1* or *BRCA2* mutations, some tumors that become resistant to platinum agents carry a reversion mutation that partially or completely restores BRCA1 or BRCA2 function and restores homologous recombination (26, 27, 34).

Reversion has also been seen in a cell line with a *BRCA2* mutation selected for PARP inhibitor resistance (27). Reversion mutations and *in cis* compensating mutations were observed in patients with Fanconi anemia, resulting in improvement in their bone marrow function (35). Inactivation of TP53BP1 restores the balance between homologous recombination and nonhomologous end joining in *BRCA1*-mutated cells and renders them resistant to PARP inhibitors (36, 37). Finally, drug transporters may prevent accumulation of platinum agents in tumor cells (38). Therefore, reversion of or compensation for a preexisting DNA repair defect may generate a tumor with high N_{tAI} but resistance to platinum treatment; other platinum resistance mechanisms unrelated to DNA repair would have the same effect.

Our analysis begins to suggest an outline of the molecular taxonomy of TNBC and ovarian cancer with respect to DNA repair and drug sensitivity. Most platinum-resistant breast or ovarian cancers are tumors with repair proficiency and low N_{tAI}. Two subsets of wtBRCA tumors possess high N_{tAI} and are sensitive to platinum-containing drugs. In one of these subsets, repair deficiency may be the consequence of low BRCA1 expression and, in the other subset, repair may be crippled by mechanisms that do not depend upon BRCA1 expression. These observations will no doubt be further refined; inclusion of reversion mutations, compensations by other events in DNA repair pathways, other mechanisms of drug resistance, and other as-yet unappreciated factors may help to enhance our prediction of drug sensitivity in the future.

In conclusion, a summary measure of telomeric chromosome aberrations in the tumor genome, N_{tAI}, predicts sensitivity to platinum treatment. Our findings implicate N_{tAI} as a marker of impaired DNA double-strand break repair. Assays to determine N_{tAI} are feasible via the use of formalin-fixed paraffin embedded tumor material, and recent algorithms such as ASCAT permit the accurate determination of copy number and AI in a majority of samples despite low tumor cell content. N_{tAI} may prove useful in predicting response to a variety of therapeutic strategies exploiting defective DNA repair.

Published OnlineFirst on March 22, 2012; DOI:10.1158/2159-8290.CD-11-0206

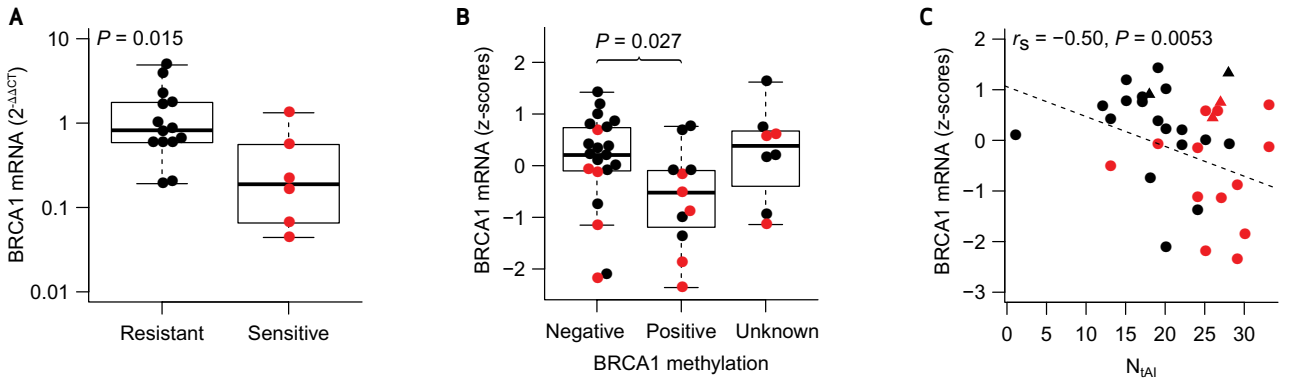

Figure 5. Association between BRCA1 transcript level and cisplatin sensitivity, *BRCA1* promoter methylation, and N_{tAI}. Red indicates tumors sensitive to cisplatin. Tumors with a germline mutation in *BRCA1* or *BRCA2* are excluded in **A** and **B** but included in **C,** represented as triangles. In **B** and **C,** BRCA1 transcript levels measured by qRT-PCR were z-transformed and combined by centering the values and dividing by the standard deviation within each trial. **A,** BRCA1 transcripts in resistant and sensitive tumors in the Cisplatin-2 cohort. **B,** BRCA1 expression in tumors by methylation status of the *BRCA1* promoter region in the combined Cisplatin-1 and Cisplatin-2 cohorts. **C,** relationship of BRCA1 transcript level and N_{tAI} in the combined Cisplatin-1 and Cisplatin-2 cohorts.

METHODS

Cell Lines and Drug Sensitivity Assays

Breast cancer cell lines were originally obtained from American Type Culture Collection and were most recently authenticated by Promega PowerPlex 1.2 short tandem repeat profiling at the DF/HCC microarray core laboratory in September 2011. Drug sensitivity measurements in breast cancer cell lines BT20, BT549, HCC1187, HCC1143, MDA-MB-231, MDA-MB-468, HCC38, MDA-MB-453 (triple-negative), CAMA-1, MCF7, T47D (ER^+), BT474, HCC1954, and MDA-MB-361 ($HER2^+$) were originally generated for a separate study in which it was reported as "data not shown" in a recently published article (13).

To summarize in brief, cells were exposed to a series of concentrations of various chemotherapeutic agents for 48 hours. Viable cell number was quantified by the use of CellTiter 96 AQueous One Solution Cell Proliferation Assay according to the manufacturer's instructions (Promega). Drug sensitivity was quantified as the dose of drug resulting in a 50% reduction of growth (IC_{50}). We found MCF7 to be highly resistant to all of the chemotherapeutic agents tested, consistent with its reported caspase-3 deficiency and resistance to drug induced apoptosis (39). In our analyses with measures of genomic aberration, MCF7 was the only clear outlier, and for these reasons, was excluded from our analyses.

Breast Cancer Cohorts and Assessment of Therapeutic Response

For this study, subjects were included for analysis of response to cisplatin if they progressed on therapy or if they received at least 3 of 4 cycles of the planned cisplatin therapy, had received no other non-protocol therapy before surgery, and if an adequate amount of tumor was available from the pretreatment biopsy. Therapeutic response was measured with the semiquantitative Miller–Payne grading system, which estimates the percentage of reduction in invasive tumor volume and cellularity on the basis of pathologic assessment of surgical samples after therapy (40). The Cisplatin-1 trial consisted of 28 mainly sporadic TNBC patients treated with preoperative cisplatin monotherapy, of whom 4 progressed on therapy and 24 completed 4 cycles of cisplatin therapy (11). Cisplatin-2 consisted of 51 TNBC patients treated with preoperative cisplatin and bevacizumab, of which 1 patient progressed on therapy and 44 patients completed 4 cycles of cisplatin therapy before surgery (12). Two patients included in this study were taken to surgery after completing 3 cycles of cisplatin therapy because of the development of toxicity; in both cases there was no appreciable pathologic response in the excised tumor after 3 cycles of cisplatin.

Preparation of Breast Cancer Samples

For both trials, core biopsies of tumor were obtained before initiation of treatment. Adequate tumor for analysis was present for 27 of 28 subjects in Cisplatin-1 and 37 of 51 subjects in Cisplatin-2. Hematoxylin and eosin–stained tissue sections of pretreatment core-needle biopsies were examined microscopically; for all biopsies for which enrichment was deemed feasible, sections were manually microdissected with the use of an 18-gauge needle. DNA was extracted by proteinase K and RNase A digestions, phenol/chloroform extraction, and ethanol precipitation. Paired normal DNA from patients was obtained from peripheral blood lymphocytes for all cases in Cisplatin-1 and from 10 cases in Cisplatin-2.

TCGA Ovarian and Breast Cancer Cohorts

Public SNP array data, expression data, and clinical annotation data were obtained for the TCGA ovarian (19) and breast cancer cohorts from the TCGA web site (41). *BRCA1* and *BRCA2* mutation status for the ovarian cancers was obtained from cBIO data portal (42). In the ovarian cohort, we identified 218 samples with SNP data that passed ASCAT (see the section entitled "Genotyping and Copy Number Analysis"), BRCA mutation status, and interpretable clinical annotations for treatment and outcomes indicating initial treatment with adjuvant platinum-based chemotherapy, predominantly the combination of carboplatin and docetaxel. We classified "treatment sensitive" patients as those annotated as having shown a partial or complete response to initial treatment and no progression or recurrence within 6 months of initial treatment ($n = 187$); the term "treatment resistant" was applied to those annotated as having stable or progressive disease on initial therapy or disease recurrence or progression within 6 months ($n = 31$). In the breast cohort, we identified 78 samples with matched gene expression and SNP data that passed ASCAT, which were classified as $ER^-/HER2^-$ on the basis of clustering of the ESR1 and ERBB2 transcripts (see Supplementary Methods).

Published OnlineFirst on March 22, 2012; DOI:10.1158/2159-8290.CD-11-0206

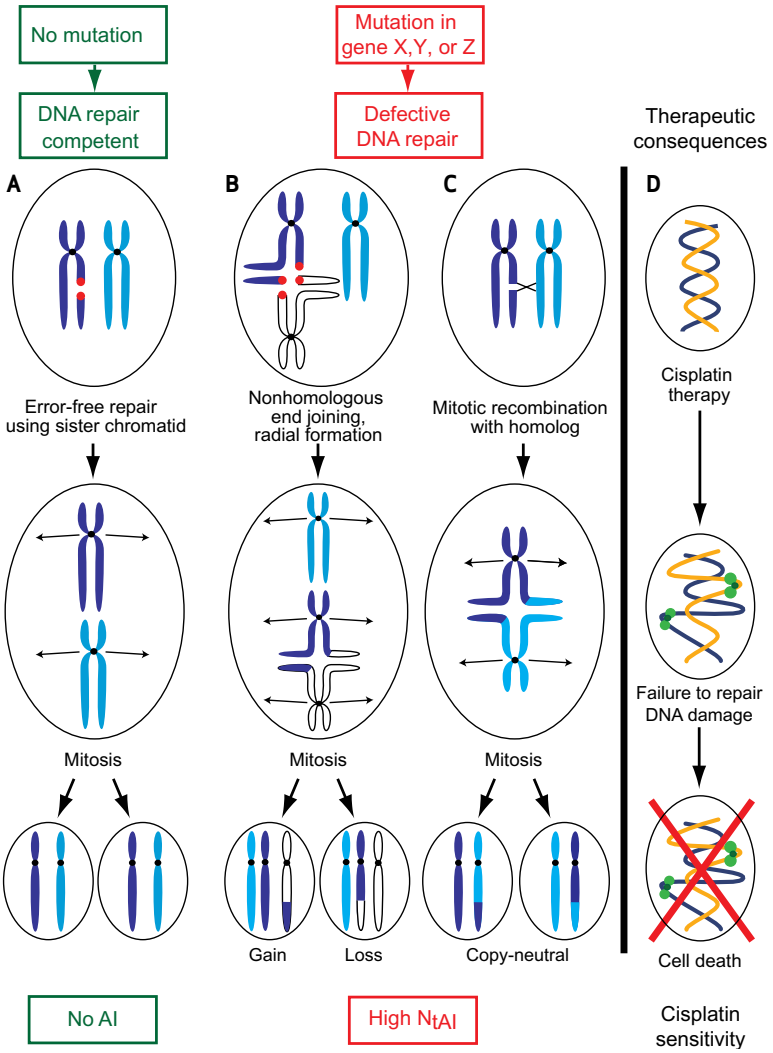

Figure 6. A model relating DNA repair to accumulation of telomeric AI and response to platinum agents. **A,** in DNA repair-competent cells, DNA breaks are repaired by the use of error-free homologous recombination employing the identical sister chromatid as a template, resulting in no AI. **B** and **C,** compromised DNA repair favors the use of error-prone repair pathways, resulting in chromosome rearrangements and aberrant radial chromosome formation. After mitotic division, daughter cells will have imbalance in the parental contribution of telomeric segments of chromosomes (telomeric AI). **B,** nonhomologous end joining is one error-prone mechanism that joins a broken chromatid of one chromosome (dark blue) to the chromatid of another, usually nonhomologous, chromosome (white). Mitotic segregation results in cells with telomeric AI as the result of monoallelic change in DNA copy number of the affected telomeric region. **C,** mitotic recombination may result in rearrangements between homologous chromosomes (dark blue and light blue). Mitotic segregation results in cells with AI because of copy neutral loss of heterozygosity. **D,** the same compromise in DNA repair that causes telomeric AI may also result in the inability of the tumor cell to repair drug-induced DNA damage, leading to tumor sensitivity to drugs such as platinum salts.

Genotyping and Copy Number Analysis

DNA was sent to Affymetrix, Inc. for determination of genotypes via use of the molecular inversion probe-based genotyping system, OncoScan FFPE Express (43). The commercial assay, which determines genotype of 330,000 SNPs, was used for analysis of the Cisplatin-2 trial. An early version of the OncoScan assay, which genotypes 42,000 SNPs, was used for the Cisplatin-1 trial. Allele signal intensity and genotypes from the OncoScan genotyping assay were processed and provided to us by Affymetrix. The OncoScan SNP genotype data for the cisplatin therapy trials were submitted to the National Center for Biotechnology Information Gene Expression Omnibus database under accession number GSE28330. Public SNP array raw data for the breast cancer cell lines were obtained from the Sanger Institute Catalogue Of Somatic Mutations In Cancer website (44, 45), public SNP array data from an independent breast cancer cell line study conducted by Heiser and colleagues (18), and public SNP array data from the TCGA ovarian (19) and breast cancer cohorts were preprocessed by the AROMAv2 and CalMaTe algorithms (46) and, when a paired normal sample was available, TumorBoost (47).

Processed genotype data from OncoScan genotyping and public SNP array data were analyzed for allele-specific copy numbers and tumor cell content by the aforementioned algorithm, ASCAT (10). ASCAT is designed to correct for normal cell contamination and tumor cell ploidy but occasionally fails to fit a model to a given sample. In this study, ASCAT failed to process 3 of 14 cell lines from Sanger, 15 of 42 cell lines from Heiser and colleagues (18), and 5 of 37 samples from the Cisplatin-2 trial. AI was defined as any time the copy number of the 2 alleles were not equal, and at least one allele was present (Supplementary Fig. S1). To ensure that all trial cases were comparable, we eliminated cases estimated by ASCAT to have less than 36% tumor cell content, the highest level of normal cell admixture in the Cisplatin-1 trial, which was the trial with an overall greater tumor purity. Thus, we included all 27 samples with SNP array data from the Cisplatin-1 trial and 26 of 32 samples with SNP array data that passed ASCAT from the Cisplatin-2 trial.

A minimum number of consecutive probes showing an aberration was required to call regions of AI and copy number change with confidence. To ensure similar aberration detection across the 3 platforms that were used, the minimum number of probes required to define a region of aberration was set to be proportional to the overall SNP density of the platform. The probe densities of the platforms were 42,000/genome OncoScan (prototype), 330,000/genome OncoScan FFPE Express, and 900,000/genome SNP6.0 for an approximate ratio of 1:8:20. Minimum probe requirements of 25 probes for 42-k OncoScan prototype, 200 probes for 330-k OncoScan FFPE Express, and 500 probes for SNP6.0 platform were chosen on the basis of

Published OnlineFirst on March 22, 2012; DOI:10.1158/2159-8290.CD-11-0206

optimizing for correlation of aberration measurement in a subset of samples with replicate data generated on both versions of the OncoScan platform (see also Supplementary Methods).

Telomeric AI and telomeric copy number change were defined as regions that extend to one of the subtelomeres but do not cross the centromere. Copy number of telomeric AI regions was defined as the mean copy number of the probes mapping to the region. Copy loss was defined as a mean of less than 1.5 copies, and copy gain was defined as a mean of greater than 2.5 copies. Association between N_{tAI} and response to cisplatin was measured by the AUC of the ROC curve for binary response. Correlation was determined by the Spearman rank correlation coefficient. Statistical significance was assessed by the Wilcoxon rank sum test. All *P* values are 2-sided.

Enrichment of CNVs at site of DNA Breakpoints

The genomic location of common CNVs was acquired from the Database of Genomic Variants (48). Mapping for HG17 and HG18 was acquired to match the SNP probe mapping of the 42-k prototype and 330-k commercial OncoScan platforms, respectively. CNVs were considered associated with a breakpoint if they overlapped within a 25-kb window on either side of the breakpoint. To test for enrichment, we performed 1,000 permutations for each cohort, where we randomly shuffled the location of the DNA breakpoints based on the location of the SNP probes, and determined how many were associated with CNVs.

BRCA1 Transcript Quantitation and Promoter Methylation Analysis

BRCA1 exon 16/17 and RPLP0 (control) qRT-PCR assay was performed as previously described (11) by the use of amplified tumor cDNA generated with the Ovation RNA Amplification System V2 kit (NuGen Technologies, Inc.). *BRCA1* promoter methylation assay was performed as previously described (11). To combine the qRT-PCR transcript data from the Cisplatin-1 and Cisplatin-2 trials, the data were z-transformed within each cohort by centering it and dividing by the standard deviation.

BRCA1 mRNA Expression in Public TCGA Cohorts

Public normalized and summarized Agilent-based gene expression data were acquired from the TCGA for all breast cancer samples (level 3). Raw Affymetrix CEL files were obtained for ovarian cancer samples (level 1). Expression data for all TCGA ovarian cancer samples were normalized and summarized by the use of robust multiarray average, and the probe set "204531_s_at" was identified as the optimum probe set for measuring BRCA1 expression with the R package "JetSet" (49).

Disclosure of Potential Conflicts of Interest

A.L. Richardson, Z. Szallasi, Z.C. Wang, D.P. Silver, A.C. Eklund, and N.J. Birkbak are inventors on a pending patent application based on this work.

Acknowledgments

The authors thank Affymetrix scientists Malek Faham, Yuker Wang, and Victoria Carlson, who performed the tumor genotype analysis of Cisplatin-1 by using an early version of OncoScan FFPE Express under a research agreement with Affymetrix, Inc.

Grant Support

This work is partly supported by the Dana-Farber/Harvard SPORE in Breast Cancer, grant number CA089393, by an Avon supplement to 5 P30 CA06516 Dana-Farber/Harvard Cancer Center Support Grant, and by the V Foundation for Cancer Research. J.E. Garber, N. Tung, Z.C. Wang. J.D. Iglehart, Z. Szallasi, and A.L. Richardson are supported by the Breast Cancer Research Foundation. N.J. Birkbak, A.C. Eklund, Q. Li, and Z. Szallasi are supported by The Danish Council for Independent Research Medical Sciences (FSS). D.P. Silver gratefully acknowledges support of the Cogan Family Foundation.

Received August 22, 2011; revised February 14, 2012; accepted February 14, 2012; published OnlineFirst March 22, 2012.

REFERENCES

1. Samouelian V, Maugard CM, Jolicoeur M, Bertrand R, Arcand SL, Tonin PN, et al. Chemosensitivity and radiosensitivity profiles of four new human epithelial ovarian cancer cell lines exhibiting genetic alterations in BRCA2, TGFbeta-RII, KRAS2, TP53 and/or CDNK2A. Cancer Chemother Pharmacol 2004;54:497–504.
2. Tassone P, Tagliaferri P, Perricelli A, Blotta S, Quaresima B, Martelli ML, et al. BRCA1 expression modulates chemosensitivity of BRCA1-defective HCC1937 human breast cancer cells. Br J Cancer 2003;88:1285–91.
3. Byrski T, Huzarski T, Dent R, Gronwald J, Zuziak D, Cybulski C, et al. Response to neoadjuvant therapy with cisplatin in BRCA1-positive breast cancer patients. Breast Cancer Res Treat 2009;115:359–63.
4. Cass I, Baldwin RL, Varkey T, Moslehi R, Narod SA, Karlan BY. Improved survival in women with BRCA-associated ovarian carcinoma. Cancer 2003;97:2187–95.
5. Turner NC, Reis-Filho JS, Russell AM, Springall RJ, Ryder K, Steele D, et al. BRCA1 dysfunction in sporadic basal-like breast cancer. Oncogene 2007;26:2126–32.
6. Sorlie T, Tibshirani R, Parker J, Hastie T, Marron JS, Nobel A, et al. Repeated observation of breast tumor subtypes in independent gene expression data sets. Proc Natl Acad Sci U S A 2003;100:8418–23.
7. Lakhani SR, Reis-Filho JS, Fulford L, Penault-Llorca F, van der Vijver M, Parry S, et al. Prediction of BRCA1 status in patients with breast cancer using estrogen receptor and basal phenotype. Clin Cancer Res 2005;11:5175–80.
8. Wang ZC, Lin M, Wei LJ, Li C, Miron A, Lodeiro G, et al. Loss of heterozygosity and its correlation with expression profiles in subclasses of invasive breast cancers. Cancer Res 2004;64:64–71.
9. Richardson AL, Wang ZC, De Nicolo A, Lu X, Brown M, Miron A, et al. X chromosomal abnormalities in basal-like human breast cancer. Cancer Cell 2006;9:121–32.
10. Van Loo P, Nordgard SH, Lingjaerde OC, Russnes HG, Rye IH, Sun W, et al. Allele-specific copy number analysis of tumors. Proc Natl Acad Sci U S A 2010;107:16910–5.
11. Silver DP, Richardson AL, Eklund AC, Wang ZC, Szallasi Z, Li Q, et al. Efficacy of neoadjuvant Cisplatin in triple-negative breast cancer. J Clin Oncol 2010;28:1145–53.
12. Ryan PD, Richardson AL, Tung NM, Isakoff S, Golshan M, Sgroi DC, et al. Neoadjuvant cisplatin and bevacizumab in triple negative breast cancer (TNBC): safety and Efficacy. J Clin Oncol 2009;27:551.
13. Li Y, Zou L, Li Q, Haibe-Kains B, Tian R, Li Y, et al. Amplification of LAPTM4B and YWHAZ contributes to chemotherapy resistance and recurrence of breast cancer. Nat Med 2010;16:214–8.
14. Silver DP, Dimitrov SD, Feunteun J, Gelman R, Drapkin R, Lu SD, et al. Further evidence for BRCA1 communication with the inactive X chromosome. Cell 2007;128:991–1002.
15. Luo G, Santoro IM, McDaniel LD, Nishijima I, Mills M, Youssoufian H, et al. Cancer predisposition caused by elevated mitotic recombination in Bloom mice. Nat Genet 2000;26:424–9.
16. Xu X, Weaver Z, Linke SP, Li C, Gotay J, Wang XW, et al. Centrosome amplification and a defective G2-M cell cycle checkpoint induce genetic instability in BRCA1 exon 11 isoform-deficient cells. Mol Cell 1999;3:389–95.
17. Vrieling H. Mitotic maneuvers in the light. Nat Genet 2001;28:101–2.
18. Heiser LM, Sadanandam A, Kuo WL, Benz SC, Goldstein TC, Ng S, et al. Subtype and pathway specific responses to anticancer compounds in breast cancer. Proc Natl Acad Sci U S A 2012;109:2724–9.

19. Bell D, Berchuck A, Birrer M, Chien J, Cramer DW, Dao F, et al. Integrated genomic analyses of ovarian carcinoma. Nature 2011;474:609–615.
20. Kolomietz E, Meyn MS, Pandita A, Squire JA. The role of Alu repeat clusters as mediators of recurrent chromosomal aberrations in tumors. Genes Chromosomes Cancer 2002;35:97–112.
21. Hastings PJ, Ira G, Lupski JR. A microhomology-mediated break-induced replication model for the origin of human copy number variation. PLoS Genet 2009;5:e1000327.
22. Iafrate AJ, Feuk L, Rivera MN, Listewnik ML, Donahoe PK, Qi Y, et al. Detection of large-scale variation in the human genome. Nat Genet 2004;36:949–51.
23. Sebat J, Lakshmi B, Troge J, Alexander J, Young J, Lundin P, et al. Large-scale copy number polymorphism in the human genome. Science 2004;305:525–8.
24. Stankiewicz P, Shaw CJ, Dapper JD, Wakui K, Shaffer LG, Withers M, et al. Genome architecture catalyzes nonrecurrent chromosomal rearrangements. Am J Hum Genet 2003;72:1101–16.
25. Hastings PJ, Lupski JR, Rosenberg SM, Ira G. Mechanisms of change in gene copy number. Nat Rev Genet 2009;10:551–64.
26. Sakai W, Swisher EM, Karlan BY, Agarwal MK, Higgins J, Friedman C, et al. Secondary mutations as a mechanism of cisplatin resistance in BRCA2-mutated cancers. Nature 2008;451:1116–20.
27. Edwards SL, Brough R, Lord CJ, Natrajan R, Vatcheva R, Levine DA, et al. Resistance to therapy caused by intragenic deletion in BRCA2. Nature 2008;451:1111–15.
28. McVean G. What drives recombination hotspots to repeat DNA in humans? Philos Trans R Soc Lond B Biol Sci 2010;365:1213–18.
29. Puliti A, Rizzato C, Conti V, Bedini A, Gimelli G, Barale R, et al. Low-copy repeats on chromosome 22q11.2 show replication timing switches, DNA flexibility peaks and stress inducible asynchrony, sharing instability features with fragile sites. Mutat Res 2010;686:74–83.
30. Richard GF, Kerrest A, Dujon B. Comparative genomics and molecular dynamics of DNA repeats in eukaryotes. Microbiol Mol Biol Rev 2008;72:686–727.
31. Cha RS, Kleckner N. ATR homolog Mec1 promotes fork progression, thus averting breaks in replication slow zones. Science 2002;297:602–6.
32. Arlt MF, Xu B, Durkin SG, Casper AM, Kastan MB, Glover TW. BRCA1 is required for common-fragile-site stability via its G2/M checkpoint function. Mol Cell Biol 2004;24:6701–9.
33. Schwartz M, Zlotorynski E, Goldberg M, Ozeri E, Rahat A, le Sage C, et al. Homologous recombination and nonhomologous end-joining repair pathways regulate fragile site stability. Genes Dev 2005;19:2715–26.
34. Swisher EM, Sakai W, Karlan BY, Wurz K, Urban N, Taniguchi T. Secondary BRCA1 mutations in BRCA1-mutated ovarian carcinomas with platinum resistance. Cancer Res 2008;68:2581–6.
35. Kalb R, Neveling K, Nanda I, Schindler D, Hoehn H. Fanconi anemia: causes and consequences of genetic instability. Genome Dyn 2006;1:218–42.
36. Bouwman P, Aly A, Escandell JM, Pieterse M, Bartkova J, van der Gulden H, et al. 53BP1 loss rescues BRCA1 deficiency and is associated with triple-negative and BRCA-mutated breast cancers. Nat Struct Mol Biol 2010;17:688–95.
37. Bunting SF, Callen E, Wong N, Chen HT, Polato F, Gunn A, et al. 53BP1 inhibits homologous recombination in Brca1-deficient cells by blocking resection of DNA breaks. Cell 2010;141:243–54.
38. Burger H, Loos WJ Eechoute K, Verweij J, Mathijssen RH, Wiemer EA. Drug transporters of platinum-based anticancer agents and their clinical significance. Drug Resist Updat 2011;14:22–34.
39. Yang XH Sladek TL Liu X, Butler BR Froelich CJ, Thor AD. Reconstitution of caspase 3 sensitizes MCF-7 breast cancer cells to doxorubicin- and etoposide-induced apoptosis. Cancer Res 2001;61:348–54.
40. Ogston KN Miller ID Payne S, Hutcheon AW Sarkar TK Smith I, et al. A new histological grading system to assess response of breast cancers to primary chemotherapy: prognostic significance and survival. Breast 2003;12:320–7.
41. The Cancer Genome Atlas [homepage on the Internet]. [cited 2011 Oct 27]. Available from: http://tcga-data.nci.nih.gov/tcga/.
42. cBioportal [homepage on the Internet]. [cited 2012 Feb 1]. Available from: http://bit.ly/wpwRXd.
43. Wang Y, Moorhead M, Karlin-Neumann G, Wang NJ, Ireland J, Lin S, et al. Analysis of molecular inversion probe performance for allele copy number determination. Genome Biol 2007;8:R246.
44. Wellcome Trust Sanger Institute [homepage on the Internet]. Available from: http://www.sanger.ac.uk/cosmic.
45. Bamford S, Dawson E, Forbes S, Clements J, Pettett R, Dogan A, et al. The COSMIC (Catalogue of Somatic Mutations in Cancer) database and website. Br J Cancer 2004;91:355–8.
46. Bengtsson H, Wirapati P, Speed TP. A single-array preprocessing method for estimating full-resolution raw copy numbers from all Affymetrix genotyping arrays including GenomeWideSNP 5 & 6. Bioinformatics 2009;25:2149–56.
47. Bengtsson H, Neuvial P, Speed TP. TumorBoost: normalization of allele-specific tumor copy numbers from a single pair of tumor-normal genotyping microarrays. BMC Bioinformatics 2010;11:245.
48. Database of Genomic Variants [homepage on the Internet]. Available from: http://projects.tcag.ca/variation/.
49. Li Q, Birkbak NJ Gyorffy B, Szallasi Z, Eklund AC. Jetset: selecting the optimal microarray probe set to represent a gene. BMC Bioinformatics 2011;12:474.